(1995); R. V. Yelle and M. A. McGrath, *Icarus* **119**, 90 (1996); E. Lelloch, in (*2*), pp. 213–242; E. Lelloch *et al.*, *Nature* **373**, 592 (1995).
5. K. S. Noll *et al.*, *Science* **267**, 1307 (1995). The Galileo Probe mass spectrometer identified H_2S in Jupiter's atmosphere (*23*).
6. S. Atreya *et al.*, in *Three Galileos: The Man, the Spacecraft, the Telescope*, J. Rahe *et al.*, Eds. (Kluwer, Dordrecht, in press).
7. K. Zahnle *et al.*, *Geophys. Res. Lett.* **22**, 1593 (1995); K. Zahnle in (*2*), pp. 183–212.
8. S. Borunov, P. Drossart, T. Encrenaz, V. Dorofeeva, *Icarus* **125**, 121 (1997).
9. There are four possible sources of H_2S for the reaction. First, impact models for the period immediately after the high-temperature explosion agree on formation of H_2S and atomic carbon (*7, 8*). Second, H_2S from the comet itself might have survived in the outer, less energized regions of the impact plume (*3*). Third, models of the jovian cloud structure predict ammonium hydroxysulfide (NH_4HS) clouds [S. K. Atreya and P. N. Romani, in *Planetary Meteorology*, G. E. Hund, Ed. (Cambridge Univ. Press, Cambridge, 1985)]. The Galileo probe nephelometer indicated tenuous clouds [B. Ragent, D. S. Colburn, P. Aurin, K. A. Rages, *Science* **272**, 854 (1996)], presumably composed of NH_4HS [(*7*); S. Atreya, private communication]. If shock waves reached these layers, reaction to ammonia, NH_3, and H_2S may have occurred [S. K. Atreya, *Atmospheres and Ionospheres of the Outer Planets and Their Satellites* (Springer, Berlin, 1986)]. And fourth, H_2S was identified in the jovian atmosphere by the Galileo probe mass spectrometer (*7, 23*).
10. Calculations used unrestricted CCSD(T) [K. Raghavachari, G. W. Trucks, J. A. Pople, M. Head-Gordon, *Chem. Phys. Lett.* **157**, 479 (1989)] in ACES II [J. F. Stanton, J. Gauss, J. D. Watts, W. J. Lauderdale, R. J. Bartlett, *Int. J. Quantum Chem. Symp.* **26**, 879 (1992)]. Triple zeta polarization (TZP) basis sets for H_2CS isomers and quadruple zeta double polarization (QZPP) [A. Schäfer, H. Horn, R. Ahlrichs, *J. Chem. Phys.* **97**, 2571 (1992)] for HCS and HSC were used for structure optimization and frequencies. Relative energies for H_2CS isomers and HCS and HSC were calculated with QZPP and QZ triple polarization (QZ3P), respectively. QZ3P used Dunning's exponents [T. H. Dunning, *ibid.* **90**, 1007 (1989)].
11. R. H. Judge, D. C. Moule, G. W. King, *J. Mol. Spectrosc.* **81**, 37 (1980); M. R. J. Hachey and F. Grein, *Chem. Phys.* **197**, 61 (1995).
12. Enthalpies of formation $\Delta H_{f^\circ(HCS)}$ are calculated as follows: $\Delta H_{R^\circ} = \Delta H_{f^\circ(HCS)} + \Delta H_{f^\circ(H)} - \Delta H_{f^\circ(H2S)} - \Delta H_{f^\circ(C)}$.
13. B. Ruscic and J. Berkowitz, *J. Chem. Phys.* **98**, 2568 (1993).
14. Y. T. Lee, *Science* **236**, 793 (1987). Peak velocities of carbon beams were determined to be 2980 and 1730 ms^{-1}, and those of the H_2S beams were 830 and 880 ms^{-1}.
15. R. I. Kaiser and A. G. Suits, *Rev. Sci. Instrum.* **66**, 5405 (1995).
16. E. A. Entenmann, thesis, Harvard University, Cambridge, MA (1966).
17. Upper limits of HSC are 10%.
18. W. B. Miller, thesis, Harvard University, Cambridge, MA (1969). The rotational period of the decomposing H_2CS acts as a clock in the experiment to estimate its lifetime.
19. The dynamics leading to the thiohydroxycarbene are governed by the addition of C(^3P_j) to H_2S to form {2}. Direct insertion into the S–H bond of H_2S to yield triplet {3} is symmetry forbidden and should have an entrance barrier larger than our lowest collision energy. The S atom and narrow 6.2 kJ mol^{-1} singlet-triplet gap of {1} and {2} could induce intersystem crossing (ISC) followed by H migration to {4}/{5}. Alternatively, {2} could undergo H migration to {3} and ISC to {4}/{5}.
20. R. I. Kaiser, C. Ochsenfeld, M. Head-Gordon, Y. T. Lee, A. G. Suits, *Science* **274**, 1508 (1996).
21. J. Moses, in (*2*), p. 243.
22. B. J. Conrath, in (*2*), pp. 293–307.
23. H. B. Niemann *et al.*, *Science* **272**, 846 (1996).
24. R.I.K. and C.O. thank the Deutsche Forschungsgemeinschaft (DFG) for Habilitation and postdoctoral fellowships, respectively. R.I.K. further thanks D. Gerlich and Y.T.L. for support. M.H.G. acknowledges a Packard fellowship. We acknowledge useful comments from S. K. Atreya, J. F. Stanton, and P. Casavecchia and discussions with M. F. A'Hearn and K. S. Noll. This work was supported by the U.S. Department of Energy.

30 October 1997; accepted 15 January 1998

Direct Observation of Heterogeneous Chemistry in the Atmosphere

Eric E. Gard, Michael J. Kleeman, Deborah S. Gross,
Lara S. Hughes, Jonathan O. Allen, Bradley D. Morrical,
David P. Fergenson, Tas Dienes, Markus E. Gälli,
Robert J. Johnson, Glen R. Cass,* Kimberly A. Prather*

The heterogeneous replacement of chloride by nitrate in individual sea-salt particles was monitored continuously over time in the troposphere with the use of aerosol time-of-flight mass spectrometry. Modeling calculations show that the observed chloride displacement process is consistent with a heterogeneous chemical reaction between sea-salt particles and gas-phase nitric acid, leading to sodium nitrate production in the particle phase accompanied by liberation of gaseous HCl from the particles. Such single-particle measurements, combined with a single-particle model, make it possible to monitor and explain heterogeneous gas/particle chemistry as it occurs in the atmosphere.

Airborne particles have an important influence on Earth's radiation balance that can lead to climate forcing (*1*). In addition, they are responsible for much of the visibility reduction observed in urban areas and national parks (*2*) and can adversely affect human health (*3*). These particles are introduced directly into the atmosphere from natural activities (for example, sea spray and volcanic eruptions) and anthropogenic pollution sources. As they evolve in the atmosphere, their chemical and physical properties—and hence their characteristics, such as light scattering and toxicity—change by accumulation of atmospheric gas-phase chemical reaction products or through heterogeneous reactions with gas-phase species. For example, gaseous sulfur dioxide emitted from fossil fuel combustion, as well as organic species emitted from both anthropogenic and biogenic sources, can react in the atmosphere to form particulate sulfates (*4*) or secondary organic aerosols (*5*), respectively. Additionally, gas-phase emissions of nitrogen oxides from combustion sources undergo homogeneous atmospheric reactions to produce gaseous species including N_2O_5 and HNO_3 (*6, 7*). These gases can diffuse to the surface of sea-salt particles where heterogeneous reactions can lead to chloride displacement from sodium chloride–containing particles, for example, by

$$HNO_{3(g)} + NaCl_{(s\ or\ aq)} \rightarrow NaNO_{3(s\ or\ aq)} + HCl_{(g)} \qquad (1)$$

(subscripts g, s, and aq refer to gaseous, solid, and aqueous phase species, respectively), leaving sodium nitrate in the particle phase (*8*).

In order to assess the effect of airborne particles on atmospheric processes, the primary particle emissions, secondary particle formation processes, and relevant heterogeneous chemistry must be understood theoretically and confirmed experimentally. The reactant-product relations involved in the heterogeneous chemistry of aerosols are generally inferred from bulk samples of atmospheric particles collected on filters or on cascade impactor substrates. Unfortunately, atmospheric particulate matter is a complex mixture of particles of many different sizes and chemical compositions, and therefore, the exact chemical speciation of the individual particles cannot be determined by bulk filter analysis. For example, if sulfate, nitrate, sodium, and ammonium ions are all present in a bulk sample, one cannot distinguish whether all particles contain each chemical species or whether pure ammonium sulfate particles coexist with pure sodium nitrate particles in the same air mass.

E. E. Gard, D. S. Gross, B. D. Morrical, D. P. Fergenson, T. Dienes, M. E. Gälli, K. A. Prather, Department of Chemistry, University of California, Riverside, CA 92521, USA.

M. J. Kleeman, L. S. Hughes, J. O. Allen, R. J. Johnson, G. R. Cass, Department of Environmental Engineering Science, California Institute of Technology, Pasadena, CA 91125, USA.

*To whom correspondence should be addressed. E-mail: glen@eql.caltech.edu; prather@citrus.ucr.edu

Recently, a number of techniques have been developed that are capable of measuring the size and chemical composition of airborne particles at the single-particle level (*9, 10*). By observing the time-evolution of the chemical species found within a population of aerosol particles as they undergo heterogeneous gas/particle chemical reactions in the troposphere, the reactant/product relations can be deduced. These relations can be confirmed by the use of an atmospheric transport and reaction model that tracks individual chemically distinct particles (*11*). In this work, we study the heterogeneous chemistry of sea-salt particles as it occurs in the ambient atmosphere by combining a single-particle model with a single-particle measurement technique.

To experimentally observe heterogeneous chemical processes at the single-particle level in the atmosphere, we conducted a field study during the fall of 1996 in California's South Coast Air Basin, which surrounds the greater metropolitan Los Angeles area. In order to measure particle transformations that occur as air parcels are advected inland from the Pacific Ocean and across the pollutant emission sources in the Los Angeles area (*12*), three aerosol monitoring stations were established: a coastal site at Long Beach, and inland sites at Fullerton and Riverside. Each site was equipped with an aerosol time-of-flight mass spectrometer (ATOFMS)—capable of determining the size and chemical composition of single particles—along with filter-based particle samplers, cascade impactors, and electronic particle size distribution monitors.

Here we focus on the replacement of chloride by nitrate in sea-salt particles (reaction 1) observed at Long Beach. This heterogeneous reaction plays an important role in atmospheric chemistry because it is a permanent sink for gas-phase nitrogen oxide species. Reaction 1 is one of the most extensively studied heterogeneous chemical reactions in the laboratory and has been investigated with a wide variety of techniques (*13*). These laboratory experiments have provided significant insight into the mechanisms, kinetics, and thermodynamics of the reaction, but none of these experiments can be certain of exactly duplicating atmospheric conditions.

The details of the transportable ATOFMS instrument used in the Southern California experiments are presented elsewhere (*9*). Briefly, particles are sampled directly from the ambient atmosphere into the ATOFMS through a convergent nozzle and accelerated to a terminal velocity, which decreases as their aerodynamic diameter increases. From this measured velocity, each particle's aerodynamic diameter is determined. Subsequent laser desorption and ionization of each particle in the source region of the coaxial reflectron time-of-flight mass spectrometer generates ions from which the chemical composition of these desorbed species can be inferred. Thus, both the size and chemical composition are obtained at the individual particle level, and by sampling many particles consecutively, the properties of the atmospheric particle mixture can be defined as it changes over time.

The transportable ATOFMS instrument, located in Long Beach (~2 miles inland from the Pacific Ocean), was operated nearly continuously in the positive-ion mode on 24 and 25 September 1996. As expected, given the site's proximity to the ocean, sea-salt particles were abundant and readily identified by the presence of Na^+ (mass-to-charge ratio $m/z = 23$), K^+ ($m/z = 39$), $Na_2{}^{35}Cl^+$ ($m/z = 81$), and $Na_2{}^{37}Cl^+$ ($m/z = 83$) peaks in their mass spectra (*14*).

The temporal variation of chloride (Cl^-) and nitrate ($NO_3{}^-$) in sea-salt particles was evident from changes in the relative intensities of their mass spectral markers with time. Because positive-ion mass spectra were obtained, positive-ion markers indicating the presence of chloride and nitrate (which normally appear as negative ions) were required. The relevant markers are Na_2Cl^+ ($m/z = 81$ and 83) and $Na_2NO_3{}^+$ ($m/z = 108$), respectively (Fig. 1). The relative intensities of Na_2Cl^+ and $Na_2NO_3{}^+$ in individual sea-salt particles were monitored continuously and subsequently averaged in 1-hour time bins; this time resolution was chosen to match that of the model used to interpret the data. Diurnal trends in the chloride and nitrate content of the particles were immediately evident when the average relative intensities of these peaks were plotted versus time (Fig. 2A).

The atmospheric chemistry occurring at Long Beach was studied with the use of a recently developed atmospheric particle formation and transport model (*10*). This model is capable of tracking aerosol processes that occur at the single-particle level in cases where the atmospheric mixture contains many particle types having distinctly different chemical properties for particles of the same size (*15*). Model calculations be-

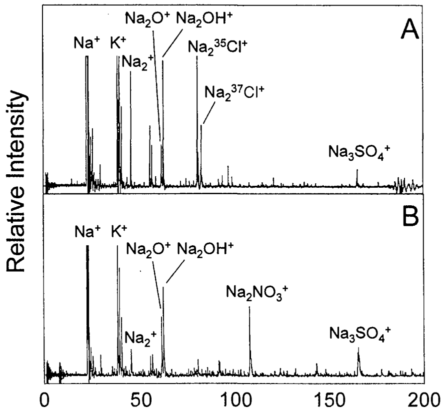

Fig. 1. (**A**) Positive-ion mass spectrum [relative ion signal intensity versus mass-to-charge ratio (m/z)] of a 2.1-μm-diameter sea-salt particle acquired at Long Beach, California, on 24 September 1996 at 20:21 PST. Na^+, K^+, Na_2Cl^+, and other Na-containing cluster ions are labeled; some additional peaks are not labeled to avoid congestion. The significant signal for the Na_2Cl^+ ion indicates that the particle is largely unreacted. (**B**) Positive-ion mass spectrum of a 1.9-μm-diameter sea-salt particle acquired at Long Beach on 24 September 1996 at 08:01 PST. Na^+ and K^+ are clearly present, as in (A); however, the Na_2Cl^+ cluster peak is undetectable, and a peak due to $Na_2NO_3{}^+$ is now present. This prominent signal due to $Na_2NO_3{}^+$ indicates that the sea-salt particle has undergone extensive reaction, in which the chloride was replaced by nitrate, forming $NaNO_{3(s\ or\ aq)}$ and releasing the chlorine as $HCl_{(g)}$. $Na_3SO_4{}^+$ peaks are evident in both spectra and are likely due to the natural abundance of sulfate in sea water.

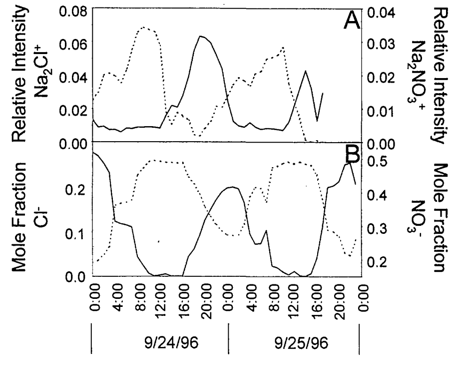

Fig. 2. A strong diurnal trend in chloride replacement by nitrate on sea-salt particles. The solid curves represent the average intensity of chloride (or chloride marker) in the particles, and the dashed line indicates the average intensity of nitrate (or nitrate maker) in the particles. (**A**) The particles analyzed by the ATOFMS over the 2-day period are sorted by their mass spectral signature, to retain only sea-salt particles. These sea-salt particles were grouped into 1-hour time bins, and the relative peak area of the chloride and nitrate marker ions, Na_2Cl^+ and $Na_2NO_3{}^+$, respectively, was determined in each single-particle mass spectrum. The average relative area for both Na_2Cl^+ and $Na_2NO_3{}^+$ was then determined for all sea-salt particles in each 1-hour time bin and plotted versus time (PST). (**B**) The time evolution of the mole fraction of chloride ion and nitrate ion in the summation of the single sea-salt particles tracked by the model calculations is plotted versus time (PST).

gin over the ocean with a captive air parcel containing gases and particles representative of regional background conditions. Additional sea-salt particles, generated by breaking surf, are inserted into the model as the air parcel crosses the coastline. As an air parcel is advected over land, pollutant gases and particles having the size distribution and chemical composition of the major urban source types (sources include motor vehicle traffic, industrial fuel combustion, and fugitive dust sources) are emitted into the air parcel. Gas-phase thermochemical and photochemical reactions lead to the production of sulfuric acid, nitric acid, and organic reactants that can form secondary aerosols or react with existing particles. Heterogeneous reactions are calculated by following the diffusion of gases to and from the particles along with the thermodynamic conditions that drive gas-particle interchange. Particles of different sizes and chemical compositions from different sources interact with common gas-phase conditions at any time, but each particle maintains a separate evolutionary history. Thus, the marine sea-salt particles can be followed separately from all other particles in the atmosphere, providing an opportunity for direct comparison with the experimental results described above.

The mechanistic air quality model was applied to the conditions observed at Long Beach during the September 1996 experiments. The paths followed by the air parcels that arrived at Long Beach at each hour of this 2-day period were computed by backward integration through hourly wind fields [calculated from wind speed and direction observations made at 28 sites in the Los Angeles area (*16*)]. Particle evolution was tracked along 48 trajectories (for examples, see Fig. 3), and the conditions observed at the end of each of these trajectories were linked to form a time series of model predictions at Long Beach (*17*). Nitric acid vapor production, both during the day and at night, is one of the many processes tracked by the model. The gas-phase HCl and HNO_3 concentrations in the South Coast Air Basin are typically at levels that drive the thermodynamically favorable displacement of chloride by nitrate in sea-salt particles (reaction 1). The extent to which this occurs is affected by many factors, including gas-phase concentrations, particle-phase concentrations, temperature, relative humidity, and reaction time.

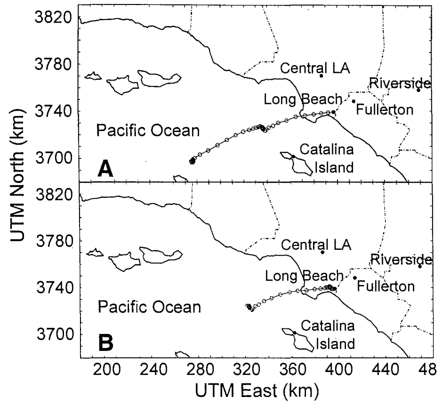

Fig. 3. Calculated air parcel trajectories for air masses arriving at the Long Beach sampling site (**A**) on 24 September 1996 at 20:00 PST, where the particles are largely unreacted because of their recent advection inland from the relatively clean offshore conditions, and (**B**) on 25 September 1996 at 09:00 PST, where the particles have exchanged a significant fraction of chloride for nitrate during the air mass stagnation over land. Both trajectories originate over the ocean at the beginning of the day before their arrival at Long Beach; the circles show the position of the air parcel at each hour, and the overlapping circles at Long Beach in (B) show air stagnation at that site. The spatial coordinates used refer to the Universal Transverse Mercator (UTM) system; the geographical region of interest falls into UTM zone 11.

To compare the model results to the ATOFMS data, we isolated the sea-salt particles having aerodynamic diameters less than 2.5 μm from those of anthropogenic origin within each trajectory calculation (*18*). For each air parcel arriving at Long Beach, the average mole fraction of Cl^- and NO_3^- in sea-salt particles was calculated. Model results show a strong diurnal variation, with chloride and nitrate being anticorrelated (Fig. 2B), which is in reasonable qualitative agreement with the trends observed by the ATOFMS.

By knowing the history of each air parcel trajectory, we can interpret the ATOFMS and model results and account for the observed diurnal cycle. The key factor determining the chloride and nitrate oscillations is the amount of time the particles spend in the polluted urban atmosphere. The relative concentration of chloride in sea-salt particles peaks from the late afternoon until the middle of the night hours of each day. The air parcels arriving in Long Beach during this period are swiftly transported from the coastline (Fig. 3A), providing little time for chloride displacement to occur. In contrast, during the late morning to early afternoon of each day, when sodium nitrate predominates, the air parcels present at the sampling site are those that have stagnated over land during the night and early morning hours (Fig. 3B). This stagnation allows time for HNO_3 production from the anthropogenic NO_x and hydrocarbon emissions, along with diffusion of the reaction products to and from the particles, permitting the chloride displacement reaction to approach completion. At the time of the experiment, meteorological data show that the same air mass stagnated over the Long Beach sampling site for 11 hours [from approximately 24:00 Pacific Standard Time (PST) on 24 September to 11:00 PST on 25 September 1996].

Thus, by monitoring the changes in the chemical composition of individual particles continuously, including measurements made within a single stagnant air mass over a period of nearly half a day, we have observed the heterogeneous conversion of sodium chloride to sodium nitrate within a population of atmospheric gas and particle-phase species. The combination of single-particle measurements and a model that can track the transformations of specific particles within a complex mixture now makes it feasible to observe, predict, and explain heterogeneous gas and particle chemistry at the single-particle level as it occurs in the atmosphere, providing a new approach to the study of atmospheric chemistry.

REFERENCES AND NOTES

1. R. J. Charlson *et al.*, *Science* **255**, 423 (1992); J. E. Penner *et al.*, *Bull. Am. Meteorol. Soc.* **75**, 375 (1994).
2. National Research Council, *Protecting Visibility in National Parks and Wilderness Areas* (National Academy Press, Washington, DC, 1993).
3. "Air Quality Criteria for Particulate Matter," *EPA/600/P-95/aF-cF* (U.S. Environmental Protection Agency, Research Triangle Park, NC, 1996).
4. J. G. Calvert *et al.*, *Atmos. Environ.* **12**, 197 (1978); J. G. Calvert and W. R. Stockwell, in *SO_2, NO, and NO_2 Oxidation Mechanisms: Atmospheric Considerations*, J. G. Calvert, Ed. (Butterworth, Boston, 1984), pp. 1–62.
5. D. Grosjean, in *Ozone and Other Photochemical Oxidants* (National Academy of Sciences, Washington, DC, 1977), pp. 45–125; S. N. Pandis *et al.*, *Atmos. Environ. A* **26**, 2269 (1992); J. R. Odum, T. P. W. Jungkamp, R. H. Griffin, R. C. Flagan, J. H. Seinfeld, *Science* **276**, 96 (1997).
6. B. J. Finlayson-Pitts and J. N. Pitts Jr., *Atmospheric Chemistry: Fundamentals and Experimental Techniques* (Wiley, New York, 1986).
7. J. H. Seinfeld, *Atmospheric Chemistry and Physics of Air Pollution* (Wiley, New York, 1986).
8. See, for example, A. R. Ravishankara, *Science* **276**, 1058 (1997); S. Langer, R. S. Pemberton, B. J. Finlayson-Pitts, *J. Phys. Chem. A* **101**, 1277 (1997); R. Vogt, P. J. Crutzen, R. Sander, *Nature* **383**, 327 (1996); A. A. P. Pszenny *et al.*, *Geophys. Res. Lett.* **20**, 699 (1993); (*6*).
9. E. E. Gard *et al.*, *Anal. Chem.* **69**, 4083 (1997) and references therein.
10. D. M. Murphy and D. S. Thomson, *J. Geophys. Res.* **102**, 6341 (1997); P. G. Carson, M. V. Johnston, A. S. Wexler, *Aerosol Sci. Technol.* **26**, 291 (1997); M. Weiss, P. J. T. Verheijen, J. C. M. Marijnissen, B. Scarlett, *J. Aerosol Sci.* **28**, 159 (1997); P. Reilly, R. Gieray, M. Yang, W. Whitten, J. M. Ramsey, *Anal. Chem.* **69**, 36 (1997); K. P. Hinz, R. Kaufman, B. Spengler, *Aerosol Sci. Technol.* **24**, 233 (1996).
11. M. J. Kleeman *et al.*, *J. Geophys. Res.* **102**, 21355 (1997).
12. L. Hughes *et al.*, in preparation.
13. See, for example, P. Beichert and B. J. Finlayson-Pitts, *J. Phys. Chem.* **100**, 15218 (1996); R. Vogt *et al.*, *Atmos. Environ.* **30**, 1729 (1996); R. Karlsson and E. Ljungstrom, *J. Aerosol Sci.* **26**, 39 (1995); M. T. Leu, R. S. Timonen, L. F. Keyser, Y. L. Yung, *J. Phys. Chem.* **99**, 13203 (1995); R. Vogt and B. J. Finlayson-Pitts, *Geophys. Res. Lett.* **21**, 2291 (1994); J. M. Laux, J. C. Hemminger, B. J. Finlayson-

Pitts, *ibid.*, p. 1623; F. F. Fenter, F. Caloz, M. J. Rossi, *J. Phys. Chem.* **98**, 9801 (1994); W. Behnke, V. Scheer, C. Zetzsch, *J. Aerosol Sci.* **24**, S115 (1993); Y. Mamane and J. Gottlieb, *ibid.* **21**, S225 (1990); B. J. Finlayson-Pitts, M. J. Ezell, J. N. Pitts Jr., *Nature* **337**, 241 (1989); F. Bruynseels and R. Van Grieken, *Atmos. Environ.* **19**, 1969 (1985).

14. To confirm that the particles selected are in fact sea salt, the ratio of the relative intensities of Na^+ and K^+ can be compared to that in sea water with use of the empirical relative sensitivity factor (RSF) measured by D. S. Gross, M. E. Gälli, and K. A. Prather (in preparation). Although the sea-salt particles are identified strictly on the basis of composition, they also have a characteristic aerodynamic diameter greater than 1.0 μm, which helps corroborate their source.
15. Previous models of urban aerosol properties as a computational approximation generally treat all atmospheric particles of the same size as having the same chemical composition and thus cannot differentiate sea-salt particles explicitly from other particles of similar size. See (*10*) for a discussion of the representation of particle size and composition in modeling calculations.
16. W. R. Goodin *et al.*, *J. Appl. Meteorol.* **18**, 761 (1979).
17. Within the model, the air parcels begin over the ocean with regional background aerosol as measured during the Southern California Air Quality Survey (SCAQS) experiments conducted in Los Angeles in 1987, and they pick up sea-salt aerosol at the concentrations measured during SCAQS as they cross the surf zone at the coastline (*10*). As the air parcels pass over land, emissions from the urban sources in Los Angeles are inserted into the model on the basis of the 1996 emissions inventory maintained by the South Coast Air Quality Management District, modified according to the procedures of A. Eldering and G. R. Cass [*J. Geophys. Res.* **101**, 19343 (1996)]. The same initial conditions for sea salt are used for each trajectory even though there must be hour-to-hour variations; for that reason, we do not expect exact agreement between predictions and observations at Long Beach.
18. The upper limit of 2.5 μm for particle diameter was chosen as the best match between the size bins used to track particles in the model calculation and the inherent transmission efficiency of the ATOFMS inlet nozzle, which transmits particles below ~3 μm with high efficiency.

19. We thank R. A. Carlin, D.-Y. Liu, C. A. Noble, P. J. Silva, and S. H. Wood for assistance with ATOFMS data acquisition. In addition, we are grateful to R. Williams and M. Berg at California State University at Long Beach and B. Gill at California State University at Fullerton for use of their facilities. Funding (University of California at Riverside) was provided by the California Air Resources Board (ARB contract 95-305). Funding (California Institute of Technology) was provided by grants from the U.S. Environmental Protection Agency (EPA grant R824970-01-0) and from the California Institute of Technology Center for Air Quality Analysis.

5 November 1997; accepted 20 January 1998

Atmospheric Radiocarbon Calibration to 45,000 yr B.P.: Late Glacial Fluctuations and Cosmogenic Isotope Production

H. Kitagawa* and J. van der Plicht

More than 250 carbon-14 accelerator mass spectrometry dates of terrestrial macrofossils from annually laminated sediments from Lake Suigetsu (Japan) provide a first atmospheric calibration for almost the total range of the radiocarbon method (45,000 years before the present). The results confirm the (recently revised) floating German pine chronology and are consistent with data from European and marine varved sediments, and combined uranium-thorium and carbon-14 dating of corals up to the Last Glacial Maximum. The data during the Glacial show large fluctuations in the atmospheric carbon-14 content, related to changes in global environment and in cosmogenic isotope production.

The atmospheric ^{14}C content (expressed in Δ^{14}C) (*1*) is sensitive to geomagnetic field strength and solar fluctuations (also through magnetic effects) as well as rearrangements in equilibrium between the major C reservoirs (atmosphere, ocean, and biosphere). Detailed calibration of the radiocarbon time scale into the glacial period is critical for accurate dating and a better understanding of changes in the Earth system.

Radiocarbon calibration can be performed by ^{14}C dating of samples that can also be dated by an independent, preferably absolute dating method. The ideal samples for this purpose are tree rings, which can be dated by dendrochronology. Dendro-calibrations with (for the most part) 20-year tree-ring resolution have been obtained for almost the complete Holocene, back to about 7900 B.C. for the absolute chronology and to about 9400 B.C. including a matched floating tree-ring curve (*2*).

Beyond the range of tree rings, calibration has been problematic. Radiocarbon dates of terrestrial macrofossils from annually laminated sediments can potentially provide a high-resolution record of atmospheric ^{14}C changes. However, varve chronologies have been revised several times (*3*). At present, calibration data from glacial varves provide a consistent data set back to about 11,000 B.C. (*4*–*6*). In addition, a marine calibration curve for the Late Glacial period is obtained by combined ^{14}C and U-series dates of corals (*7*, *8*) and ^{14}C measurements on foraminifera from varved marine sediments (*9*). Because these data are for marine materials, they have to be corrected for the apparent ^{14}C age of the surface oceans, known as the reservoir effect.

Here we present a high-resolution atmospheric radiocarbon calibration from annually laminated sediments for the total range of the radiocarbon dating method [<45,000 cal yr B.P. (*10*)]. The sediments were taken from Lake Suigetsu (35°35′N, 135°53′E) near the coast of the Sea of Japan (*11*). The lake is 10 km around the perimeter and covers an area of 4.3 km^2. It is a typical kettle-type lake with a nearly constant depth at the center, ~34 m deep. A 75-m-long continuous core (Lab. code, SG) and four short piston cores were taken from the center of the lake in 1991 and 1993. The sediments are laminated in nearly the entire core sections and are dominated by dark-colored clay with white layers resulting from spring-season diatom growth. The seasonal changes in the depositions are preserved in the clay as thin laminations or varves. The sedimentation or annual varve thickness is relatively uniform, typically 1.2 mm/year during the Holocene and 0.61 mm/year during the Glacial. The bottom age of the SG core is estimated to be older than 100,000 years, close to the beginning of the last interglacial period.

To reconstruct the calendar time scale, we counted varves, based on gray-scale image analyses of digital pictures, in a 10.43- to 30.45-m-deep section, producing a 29,100-year-long floating chronology. Because we estimated the varve chronology of older than ~20,000 yr B.P. (19-m depth of SG core) by counting in a single core section, the error of the varve counting increases with depth, and the accumulated error at 40,000 cal yr B.P. would be less than ~2000 years, assuming no break in the sediment (*12*).

The ^{14}C/^{12}C and ^{13}C/^{12}C ratios of more than 250 terrestrial macrofossils (leaves, twigs, and insect wings) in the sediments were measured by accelerator mass spectrometry (AMS) at the Groningen AMS facility (*13*), after proper sample pretreatment (*14*).

The floating varve chronology was connected to the old part of the absolute tree-ring chronology (*2*, *15*) by ^{14}C wiggle matching (*16*), resulting in an absolute calendar age covering the time span from 8830 to 37,930

H. Kitagawa, International Research Center for Japanese Studies, 3-2, Goryo Oeyama-cho, Nishikyo-ku, Kyoto, 610-1192 Japan.
J. van der Plicht, Centre for Isotope Research, Nijenborgh 4, 9747AG Groningen, Netherlands.

*To whom correspondence should be addressed.